Bull. Mater. Sci. (2022) 45:209
https://doi.org/10.1007/s12034-022-02789-z

Study on electrodeposition behaviour and corrosion resistance of nickel-copper alloy in ChCl-EG deep eutectic solvents

XU FU, HAIJING SUN, CHONGBO ZHAN, RUNJIA ZHANG, BAOJIE WANG and JIE SUN*

School of Environmental and Chemical Engineering, Shenyang Ligong University, Shenyang 110159, People's Republic of China

*Author for correspondence (jiersun2000@126.com)

MS received 10 April 2022; accepted 20 June 2022

Abstract. Choline chloride-ethylene glycol (ChCl-EG) deep eutectic solvents were used as the electrolytes to study the cathode reduction process. The electrochemical behaviour of nickel and copper ions in ChCl-EG, the morphology, phase composition and corrosion resistance of the coatings were characterized. The results showed that the increase in the temperature of the electrodeposition solution system can make the reduction potentials of nickel and copper ions approaching, making it easier to achieve co-deposition. When the temperature of the solution was 70°C, a nickel-copper alloy similar to the commercial Monel (Ni70Cu30) with good corrosion resistance can be obtained.

Keywords. Ionic liquid; nickel-copper alloy; corrosion resistance.

1. Introduction

Nickel-copper (Ni-Cu) alloys, especially Ni70Cu30 alloys, namely Monel alloy, are widely used in the fields of aviation, navigation, chemical industry, metallurgy and medical equipment [1]. Based on this, the use of electrodeposition on different metal surfaces to cover a layer of nickel-copper alloy has become an important means of corrosion resistance [2]. The use of traditional aqueous solution electrodeposition methods to prepare nickel-copper alloy has been relatively mature and has been widely used [3–5]. While in aqueous solution, it needs to add a large number of additives for electrodeposition, such as complexing agent, brightener, etc., to improve the quality of coating. The heavy metal ions contained in electroplating wastewater, including nickel ions and copper ions, as well as other organic substances, pose threats to health and the environment. Therefore, finding an environmentally friendly electrodeposition system has become the goal of researchers.

In recent years, ionic liquids have attracted attention in the field of metal electrodeposition due to their wide electrochemical window and high thermal stability [6–8]. In terms of using ionic liquids as base liquids for the electrodeposition of nickel-copper alloys, Deng *et al* [9], Wang *et al* [10] and Gao *et al* [11] used different ionic liquids to study the electrodeposition of nickel-copper alloys. The properties of the ligand, the composition of the alloy and the corrosion resistance of the coatings have all been studied, and meaningful results have been obtained.

Published online: 26 October 2022

In this paper, the electrochemical deposition of nickel-copper alloy was studied using choline chloride-ethylene glycol (ChCl-EG) deep eutectic solvents as the electrolytes. The electrochemical behaviour of nickel and copper ions in ChCl-EG, the morphology, phase composition and corrosion resistance of the coatings were characterized.

2. Experimental

Choline chloride ($C_5H_{14}ClNO$, ChCl), ethylene glycol ($(CH_2OH)_2$, EG), 0.05 mol l^{-1} copper chloride dihydrate ($CuCl_2{\cdot}2H_2O$) and 0.1 mol l^{-1} nickel chloride hexahydrate ($NiCl_2{\cdot}6H_2O$) used in the experiment were all analytically pure. Choline chloride and ethylene glycol were added to the beaker at a molar ratio of 1:2, and stirred at 70°C to a colourless and transparent solution. Then, copper chloride and nickel chloride were added successively and stirred for 12 h. After this process, the electrolyte was dried in an electric vacuum drying oven for 12 h, and ChCl-EG deep eutectic solvents were obtained.

The CS350 electrochemical workstation was used for electrochemical behaviour analysis and electrodeposition experiments. The electrochemical test of cyclic voltammetry (CV) adopted a three-electrode system, in which the counter electrode was a platinum electrode, the reference electrode was a silver electrode, and the working electrode was a glassy carbon electrode. In the

electrodeposition test, the working electrode was a brass sample (Cu0.64Zn0.36, 1 × 4 cm^2), The experimental temperature was 70°C. Before the electrodeposition experiments, 240#, 400#, 1200# and 2000# sandpaper were used to grind and polish the brass sample, then cleaned the test piece with acetone and put it in absolute ethanol for later use.

D/max-RB (Rigaku) 12 kW rotating target X-ray diffractometer was used to determine the phase composition of the coating (using q-2θ continuous scanning mode, step size 0.02° (2θ), scanning speed 4° (2θ) min^{-1}, copper target, voltage 40 kV, current 30 mA). Micro-morphology of the deposition coating was characterized using scanning electron microscopy (SEM, TESCAN MIRA4) coupled with energy dispersive X-ray spectroscopy (EDS), and the elemental compositions of the coating were performed using EDS analysis.

3. Results and discussion

3.1 *Cyclic voltammetry curve test and analysis*

The CV curves of (A) ChCl-EG, (B) ChCl-EG + Cu^{2+}, (C) ChCl-EG + Ni^{2+} and (D) ChCl-EG + Cu^{2+} + Ni^{2+} on the GC electrode are seen in figure 1a. The curves sweep from E = 1.5 to –1.5 V, and then to E = 1.5 V, the sweep rate is 100 mV s^{-1}, and the temperature is 70°C. It can be seen from figure 1a (curve A) that the ChCl-EG deep eutectic solvents have a wider electrochemical window, from which a smaller reduction peak Ac0 can be observed. The formation of this reduction peak Ac0 is the result of the reduction of choline cation to trimethylamine [12]. Three reduction peaks can be found in the CV curve of ChCl-EG + Cu^{2+} (curve B), among which the reduction peak Bc1 corresponds to the process of reducing Cu^{2+}→Cu^{+}, and the corresponding oxidation peak is Ba1. The reduction peak Bc2 corresponds to Cu^{+}→Cu, and the corresponding oxidation peak is Ba2. Figure 1a (curve C) shows a single reduction peak Cc1, indicating that the reduction process of Ni^{2+} is a one-step process of Ni^{2+}→Ni, corresponding to the oxidation peak Ca1. There are three reduction peaks in the CV curve (shown in figure 1a (curve D)) of ChCl-EG + Cu^{2+} + Ni^{2+}. The first reduction peak Dc0 corresponds to the reduction of choline cations, and the second reduction peak Dc1 is Cu^{2+}→Cu^{+}, the third reduction peak Dc2 is relatively close to the middle of curves B and C, corresponding to Cu^{+}→Cu and Ni^{2+}→Ni. Combining curves B and C shows that Ni and Cu are co-deposited at this potential.

Figure 1b shows the CV curves of the ChCl-EG + Cu^{2+} + Ni^{2+} system at different temperatures of 30, 50 and 70°C. The scanning rate is 100 mV s^{-1} and the scanning interval is –1.5 to 1.5 V. It can be seen that 0–1 V contains two reduction peaks in figure 1b. In combination with figure 1a, it can be known that the first reduction peak corresponds to the reduction of choline cation to trimethylamine. The other reduction peak corresponds to the first reduction of copper, namely Cu^{2+}→Cu^{+}. In figure 1b, it can be seen that at around –1.0 V, two reduction peaks appear at lower temperatures (30 and 50°C), namely Cu^{+}→Cu and Ni^{2+}→Ni, and the two reduction peaks gradually move closer. However, only one reduction peak can be observed at 70°C, which shows that increasing the temperature can make the reduction potentials of the two close, and increasing the temperature is more conducive to the co-deposition of nickel-copper alloys.

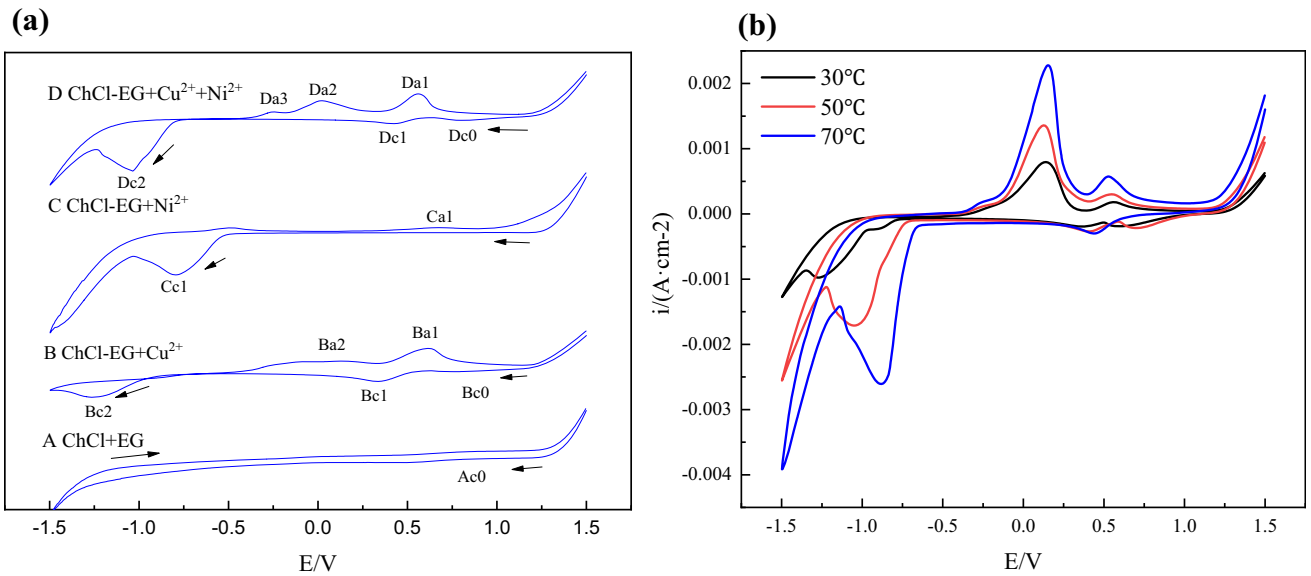

Figure 1. (**a**) Cyclic voltammetry curves of different systems. (**b**) Cyclic voltammetry curves of ChCl-Eg + Cu^{2+} + Ni^{2+} at different temperatures.

3.2 *Chronoamperometry curve test and analysis*

In order to study the nucleation and growth mechanism of nickel and copper ions in ChCl-EG deep eutectic solvents, the chronoamperometry curves obtained including nickel and copper ions were measured using glassy carbon electrode at different temperatures. The results of the experiments and the comparison with the theoretical model are shown in figure 2.

According to the different growth models, crystal nucleation can be divided into two-dimensional nucleation and three-dimensional nucleation. The theoretical model of three-dimensional nucleation growth for the electrocrystallization of metal ions in solution can be divided into instantaneous nucleation and progressive nucleation. The instantaneous nucleation refers to the formation of a large number of nucleation growth sites on the entire working electrode surface at an extremely fast rate, and then only the accumulation and growth of metal atoms are carried out on these sites. While progressive nucleation is a function of time. On the surface of the working electrode, new active sites appear continuously, and metals perform subsequent growth on the successively appeared active sites. The actual current for two-dimensional and three-dimensional nucleation can be calculated using the following functional expressions:

Two-dimensional nucleation growth:

$$i = (2\pi nFk^2MN_0ht/d)\exp(-\pi k^2M^2N_0t^2/d^2)$$

Instantaneous nucleation (1)

$$i = (\pi nFk^2MN_0bht^2/d)\exp(-\pi k^3M^2N_0bt^3/3d^2)$$

Progressive nucleation (2)

Three-dimensional nucleation growth:

$$i = (nFD^{1/2}C/\pi^{1/2}t^{1/2})[1-\exp(-N_0\pi kDt)]$$

Instantaneous nucleation (3)

$$k = (8\pi CM/d)^{1/2}$$

$$i = (nFD^{1/2}C/\pi^{1/2}t^{1/2})[1-\exp(-bN_0\pi k'Dt^2/2)]$$

Progressive nucleation (4)

$$k' = 4/3(8\pi CM/d)^{1/2}$$

where F is the Faraday constant, k is the reaction rate constant, r the radius of the formed grain, N_0 the critical grain density, M the molar mass of the deposit, h the grain height, d the density of the deposit, D the diffusion coefficient, C the concentration, and b is a constant.

As can be seen in figure 2a, the working electrode is charged with the electric double layer at a specific potential, the current continues to rise, and finally reaches the extreme value (i_{max}). Then the nickel and copper ions near the electrode surface are consumed, the concentration of metal ions in the solution decreases, the current decreases, and the reaction rate decreases accordingly, indicating that the process is controlled by diffusion.

Based on formulas (5) and (6), the chronoamperometry curves obtained under different temperature conditions are subjected to dimensionless processing, and the results are shown in figure 2b.

$$(i/i_m)^2 = [1.9542/(t/t_m)]\{1-\exp[-1.2564(t/t_m)]\}^2$$

Three-dimensional instantaneous nucleation (5)

$$(i/i_m)^2 = [1.2254/(t/t_m)]\{1-\exp[-2.3367(t/t_m)^2]\}^2$$

Three-dimensional progressive nucleation (6)

The results in figure 2b indicate that nickel-copper follows a three-dimensional instantaneous nucleation growth mechanism in this system.

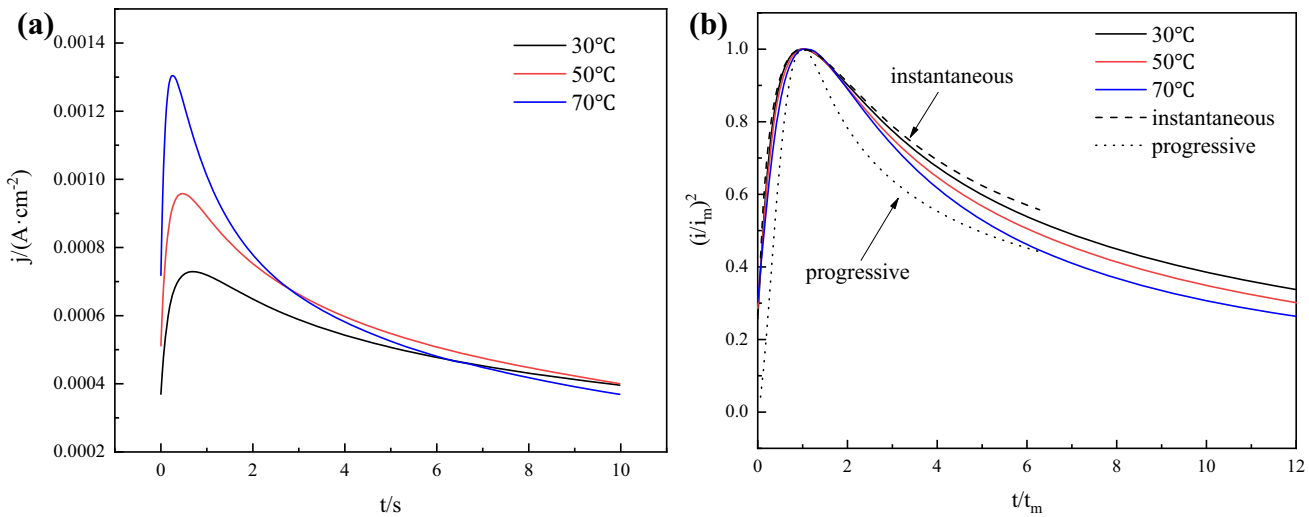

Figure 2. Chronoamperometry curve test of ChCl-EG-$CuCl_2$-$NiCl_2$ system at different temperatures.

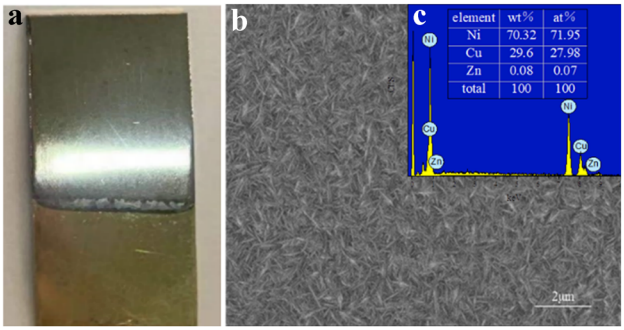

Figure 3. Morphology and elemental analysis results of the coating at 70°C.

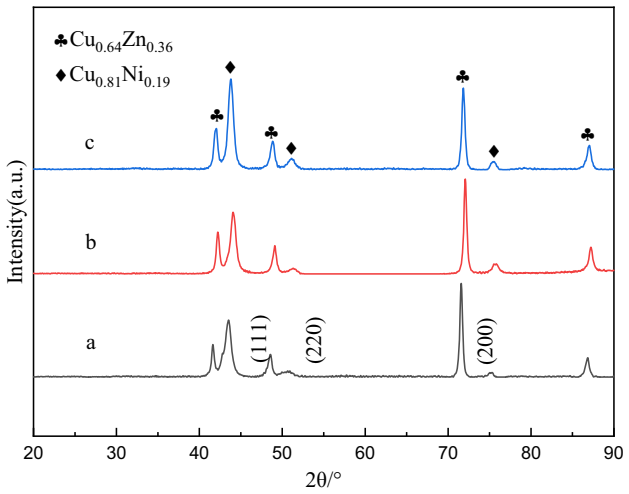

Figure 4. XRD spectrum of coating electrodeposition for 1 h: (a) 30°C, (b) 50°C and (c) 70°C.

3.3 *Surface topography and energy spectrum analysis*

Figure 3a shows the macroscopic morphology of electrodeposited coatings at –0.95 V in 1 h. It shows that the coating is bright and has obvious metallic luster. Figure 3b is a microtopography of the coating surface at 70°C. It can be seen from the figure that the brass substrate is basically covered by particles to obtain a needle-like coating, the coating is flat and uniform, and there are no bare or empty holes. It can be seen from the EDS results (figure 3c) that there is a very small amount of zinc in the coating, which proves that the coating basically covers the brass substrate. The ratio of nickel to copper in the coating is close to 7:3, which is basically the same as the Monel alloy commonly used in the industry.

3.4 *X-ray diffraction analysis*

In order to determine the effect of temperature on the phase composition of the electrodeposited coating, X-ray diffraction (XRD) tests were performed on the nickel-copper coatings at different temperatures after electrodeposition for 1 h, and the test results are shown in figure 4. It can be seen from the diffractogram that the strong substrate peak (Cu0.64Zn0.36) appears in the XRD spectrum because of the breakdown of the surface coating and hitting the substrate during the XRD test. Comparing the test results with the PDF standard card, the nickel-copper coating obtained by electrodeposition grows along the (111), (220), (200) crystal planes, and the nickel-copper coating obtained in this system is composed of a nickel-copper alloy phase Cu0.81Ni0.19 composition.

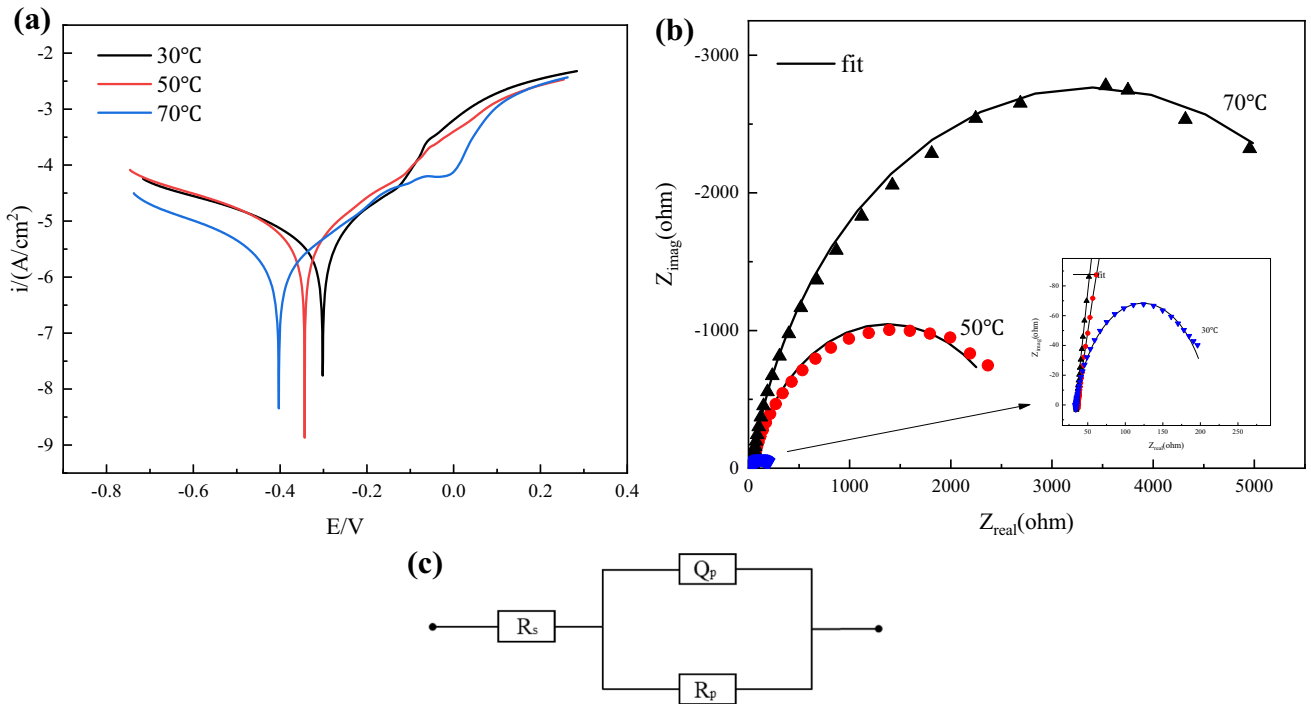

Figure 5. Tafel curve test and electrochemistry impedance test results of coatings at different temperatures.

Table 1. Corrosion parameters of Ni-Cu alloy deposits determined from polarization curves in 3.5% NaCl solution.

	i_{corr} (A cm^{-2})	E_{corr} (V)	R_s (Ω cm^2)	R_p (Ω cm^2)
30°C	6.14×10^{-6}	–0.302	34.12	178.4
50°C	6.19×10^{-6}	–0.343	36.65	2678.8
70°C	1.91×10^{-6}	–0.403	34.56	6687.6

3.5 *Analysis of the corrosion resistance of the coating*

In order to study the effect of temperature on the corrosion resistance of Ni-Cu alloy, the Tafel curve test and impedance test of Ni-Cu alloy coatings at different temperatures were tested in 3.5 wt% NaCl solution. The results of Tafel curve test are shown in figure 5a, while the specific corrosion parameters are shown in table 1. It can be concluded that the corrosion current densities of the nickel-copper alloy obtained at 30 and 50°C are 6.14×10^{-6} and 6.19×10^{-6} A cm^{-2}, respectively. When the temperature reaches 70°C, the corrosion current density of the nickel-copper alloy obtained is 1.91×10^{-6} A cm^{-2}. The corrosion characteristic of commercial Monel-400 (67Ni, 30Cu, 2Fe, 0.03C) is $i_{corr} = 2.24 \times 10^{-6}$ A cm^{-2} [13]. It can be seen from the data comparison that when the temperature reaches 70°C, a coating with corrosion resistance equivalent to that of Monel alloy can be obtained.

The electrochemical impedance test results of the Ni-Cu coating at different temperatures is shown in figure 5b. Figure 5c shows the equivalent circuit diagram, where R_s is solution resistance, R_P is charge transfer resistance, and QP is the constant phase element (CPE) whose magnitude is mainly related to the electrical properties of the double layer on the electrode surface.

From the data shown in table 1, as the temperature increases, the R_p value increases (the R_p value increases from 178.4 to 6687.6), and the best corrosion resistance of the coating was obtained at 70°C, in agreement with the results obtained from the polarization curves.

4. Conclusions

In the ChCl-EG deep eutectic solvents, the electrodeposition preparation of nickel-copper alloy coating can be carried out without the use of additives. The reduction potentials of nickel ions and copper ions are not much different, and the increase in temperature can promote the co-deposition of nickel-copper alloy, and can improve its corrosion resistance. When the electrodeposition temperature is 70°C, the composition of the coating phase is Cu0.81Ni0.19 alloy phase, the surface of the coating is bright and flat, the micro-morphology is pinpoint particles, the ratio of nickel to copper is approximately 7:3, and the corrosion resistance is equivalent to commercial Monel alloy.

Acknowledgements

This work was supported by the project of Liaoning Province-Shenyang National Laboratory for Materials Science Joint Research Fund (project No.: 2019JH3/30100021). And this work was also supported by the High-level Achievement Construction Project and Scientific Research and Innovation Team Support Project by Shenyang Ligong University.

References

[1] Baskaran I, Narayanan T S N S and Stephen A 2006 *Mater. Lett.* **60** 16
[2] Saranya D, Velayutham D and Suryanarayanan V 2014 *J. Electroanal. Chem.* **734** 70
[3] Ishikawa M, Enomoto H, Matsuoka M and Iwakura C 1995 *Electrochim. Acta* **40** 11
[4] Rajasekaran N and Mohan S 2009 *Corros. Sci.* **51** 9
[5] Kamel M M, Anwer Z M, Abdel-Salam I T and Ibrahim I S 2014 *Surf. Interface Anal.* **46** 7
[6] Qian H X, Sun J, Li Q S, Sun H J and Fu X 2020 *Electrochem. Soc.* **167** 102511
[7] Li Q S, Qian H X, Fu X, Sun H J and Sun J 2021 *Mater. Res. Bull.* **44** 1
[8] Sun J, Ming T Y, Qian H X and Li Q S 2018 *Electrochim. Acta* **297** 12
[9] Deng M J, Lin P C, Sun I W, Chen P Y and Chang J K 2009 *Electrochemistry (Tokyo)* **77** 8
[10] Wang S H, Guo X, Yang H, Dai J C, Zhu R, Gong J *et al* 2014 *Appl. Surf. Sci.* **288** 530
[11] Gao M Y, Yang C, Zhang Q B, Yu Y W, Hua Y X, Li Y *et al* 2016 *Electrochim. Acta* **215** 609
[12] Yue D, Jia Y, Ying Y, Sun J and Yan J 2012 *Electrochim. Acta* **65** 30
[13] Lin Y P and Selman J R 1993 *J. Electrochem. Soc.* **140** 1304